Electronic Supplementary Material (ESI) for Nanoscale.

Constructing Oriented Two-Dimensional fish scale-like Gd@MXene Barrier Walls in PVA to achieve Excellent neutron shielding Properties

Xinguo Zhu, Xianlong Zhang*, Shaoyun Guo

The State Key Laboratory of Polymer Materials Engineering, Polymer Research Institute of Sichuan University, Chengdu 610065, China

E-mail: 13391112759@163.com (Xinguo Zhu); zhangxianlong_1985@163.com (Xianlong Zhang); sguo@scu.edu.cn (Shaoyun Guo)

Preparation of MXene dispersants:

MXene ($Ti_3C_2T_X$) dispersions were based on previous literature synthesis. Typically, 6 g LiF powder was slowly added to a 120 mL 9M HCl solution placed in a 200 ml Teflon container and magnetically stirred for 30 min at room temperature until LiF was completely dissolved. Then, 6 g Ti_3AlC_2 powder was slowly added to the mixing solution in 10 minutes with magnetically stirring, the mixture was reacted at room temperature for 24 hours, obtaining multi-layer $Ti_3C_2T_X$, multi-layer $Ti_3C_2T_X$ by centrifugal washing (3500 rpm washing with deionized water) several times, until its pH reached 6. The multi-layer $Ti_3C_2T_X$ was then stripped of at least the layer $Ti_3C_2T_X$ by ultrasonic processing (180 W, 30 minutes). After that, centrifuge the dark green solution at 3500 rpm for 3 minutes to obtain a single-layer $Ti_3C_2T_X$ nanoflakes.

preparation of GMNFs hybrids

GMNFs were synthesized by a one-step hydrothermal reaction. First of all, a certain amount of $Gd(NO_3)_3.6H_2O$ was added to the equivalent MXene dispersant in the Teflon beaker (2.7 mg. L^{-1}, 150 ml). Then, the mixture was magnetically stirred to make Gd^{3+} fully absorbed by MXene, and then transferred the mixture from beaker to the oven for hydrothermal reaction (170 ℃, 12 h) to synthesis GMNFs. Finally, GMNFs powder was obtained by centrifugation, washing and freeze-dried. In order to study the effect of the addition of Gd^{3+} on MXene's reduction performance and neutron shielding performance of GMNFs/PVA film, remained the addition of the MXene unchanged and increased the addition of $Gd(NO_3)_3.6H_2O$ to synthesis multiple GMNFs with different content of Gd. For convenience, MXene : $Gd(NO_3)_3.6H_2O$ =1:x was named x-Gd@MXene or x-GMNFs.

Table S1 The addition of MXene and $Gd(NO_3)_3$ in different hybrids

	MXene	5-GMNFs	7.5-GMNFs	10-GMNFs	15-GMNFs	20-GMNFs
C(MXene)	1.380	1.380	1.380	1.380	1.380	1.380
C($Gd(NO_3)_3$)	0	6.933	8.667	14.717	28.167	41.333
Radio	1:0	1:5	1:7.5	1:10	1:15	1:20

Preparation of GMNFs /PVA films

First, added 15 g PVA powder to the GMNFs mixture and poured into the three-neck flask for quick stirring (95 ℃, 12 h) until the PVA was completely dissolved. The mixture was dropped onto a glass plate, and then the glass plate was placed on a spin coater to coat a uniform film. Then, the film was placed in an ethanol bath for solvent diffusion for 5 minutes, and the water of film was drained from the film. Finally, removed the film from the glass slide and collected it for later use.

The sedimentation of the filler is mainly due to that the MXene nanosheets are loaded with higher density of Gd^{3+}, and the –OH of the surface of the MXene has been oxidized, resulting in the deterioration of dispersion because of the destruction of the hydrogen bond between the water and the MXene nanosheets.

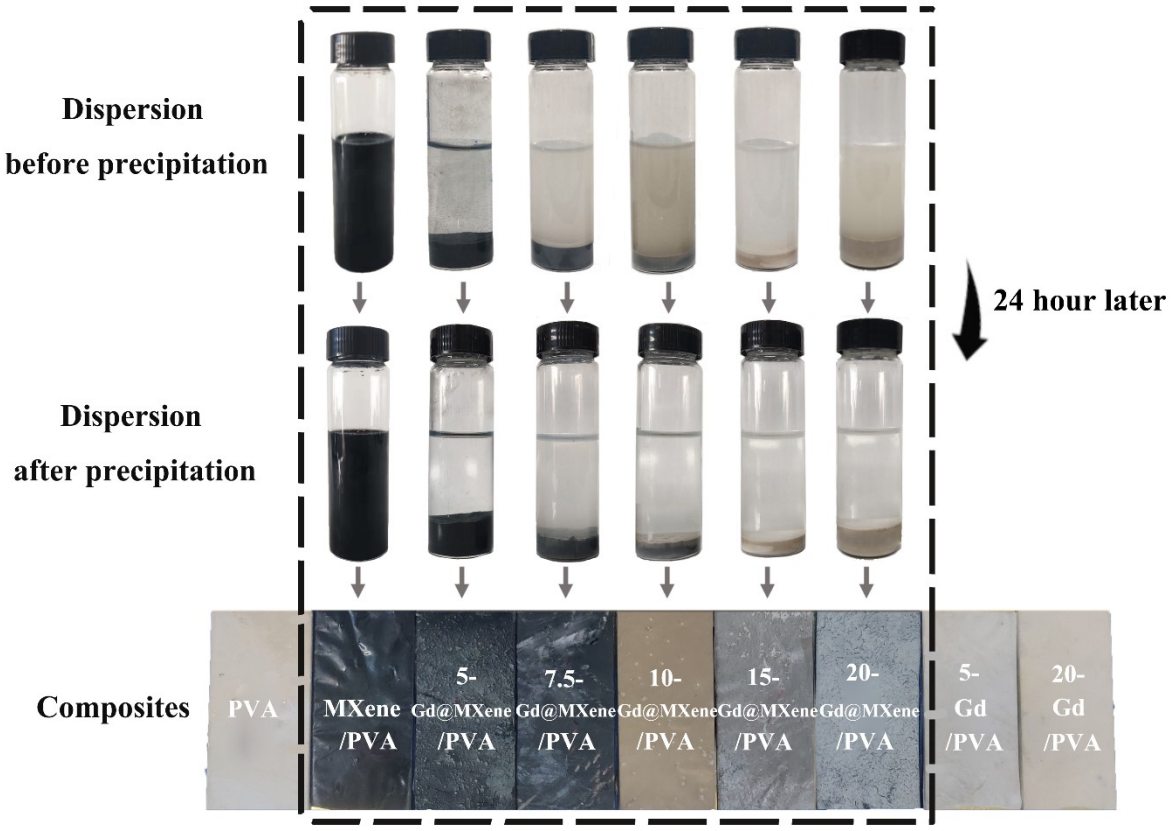

Fig. S1 (a) Digital images of MXene, 5-Gd@MXene, 10- Gd@MXene and 20- Gd@MXene. (b) Water dispersion of MXene and GMNFs. (c) The films of PVA, MXene/PVA, GMNFs/PVA, and Gd/PVA.

Neutron shielding tests

This neutron shielding test used a neutron source of Cf, test temperature was 15 ℃, relative humidity R.H.: 40%, detector: SP9 proportional count tube (4 atm), and the film thickness selected for testing was below 100 μm. The neutrons released from the source were slowed down to the thermal energy segment as the source item used in the test using the cylinder-shaped polyethylene. The detector used an SP9 proportional count tube with a high response to thermal neutron detection, an internal air pressure of 4 atm, and a high working pressure of 1000 V. The proportional count tube was surrounded by a sufficient amount of film tested to shield the neutron background caused by scattering around the experimental site. The back end

of the proportional count tu e was connected to the preamplifier 142PC and the main amplifier 570. The detector inputted signal entered the multi-channel analyzer after the preamplifier 142PC and the main amplifier 570, and outputted 1024 energy deposition spectra for data analysis. The shielding effect of shielding material on hot neutrons could be known by comparing the count rate of proportional count tube after placing shielded material with the count rate of unshielded material. To ensure statistical accuracy, the count measured in each case was guaranteed to exceed 10,000.

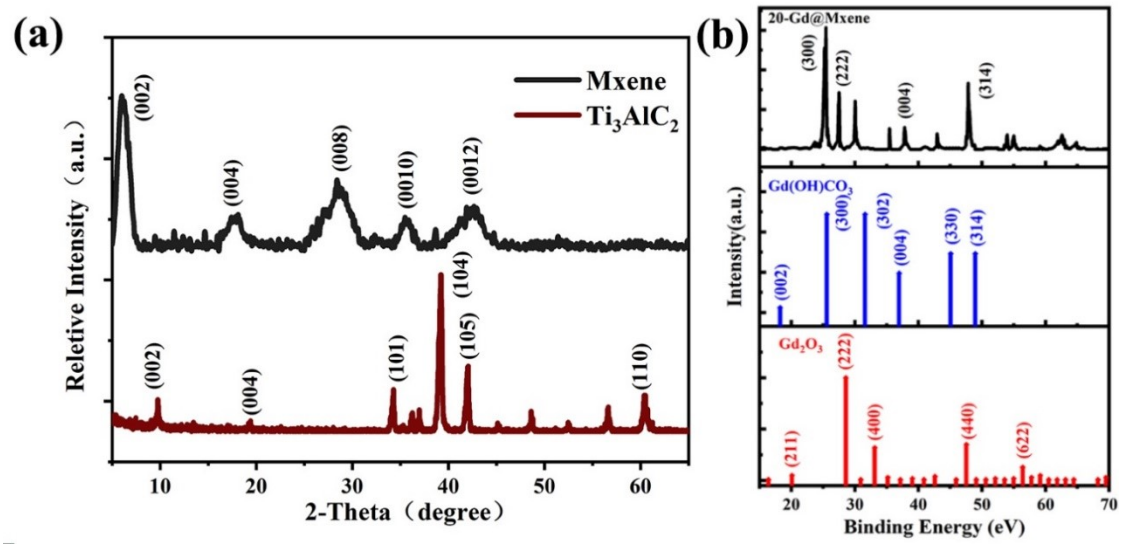

Fig. S2 (a) Comparison of XRD patterns of MXene and MAX. (b) Comparison of spectra of 20-Gd@MXene and $Gd(OH)CO_3$ and Gd_2O_3.

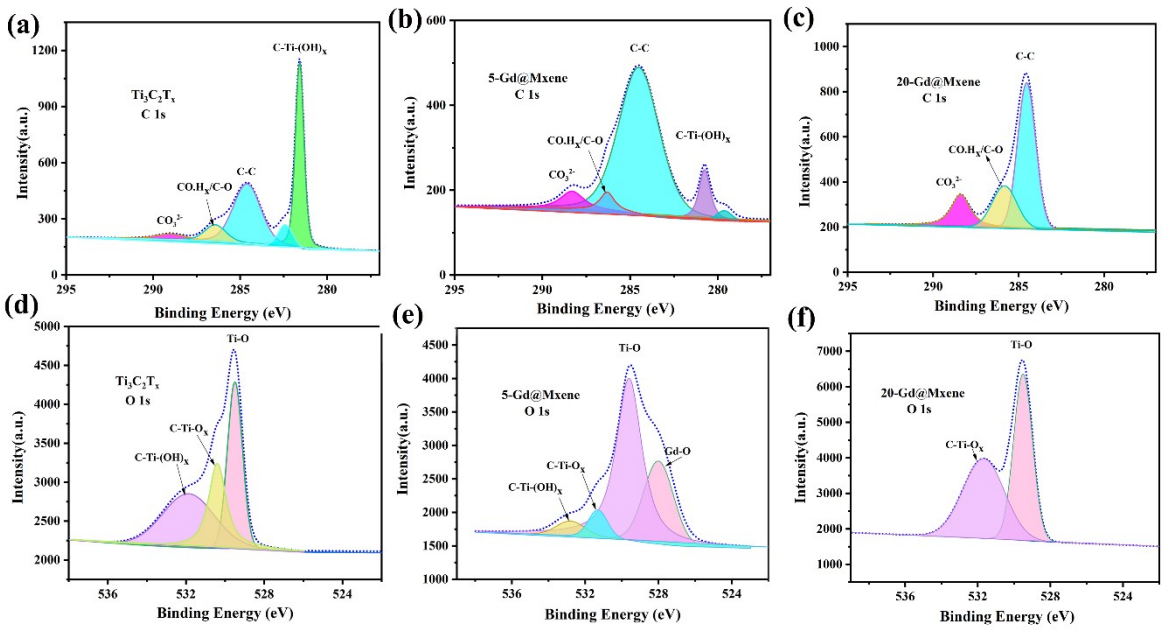

Fig. S3 High-resolution XPS spectrum of C1s of Mxene (a), 5-Gd@Mxene (b), and 20-Gd@Mxene (c). d) High-resolution XPS spectrum of Ti2p of $Ti_3C_2T_x$-Mxene. High-resolution XPS spectrum of O1S of 5-Gd@Mxene (e) and 20-Gd@Mxene (f).

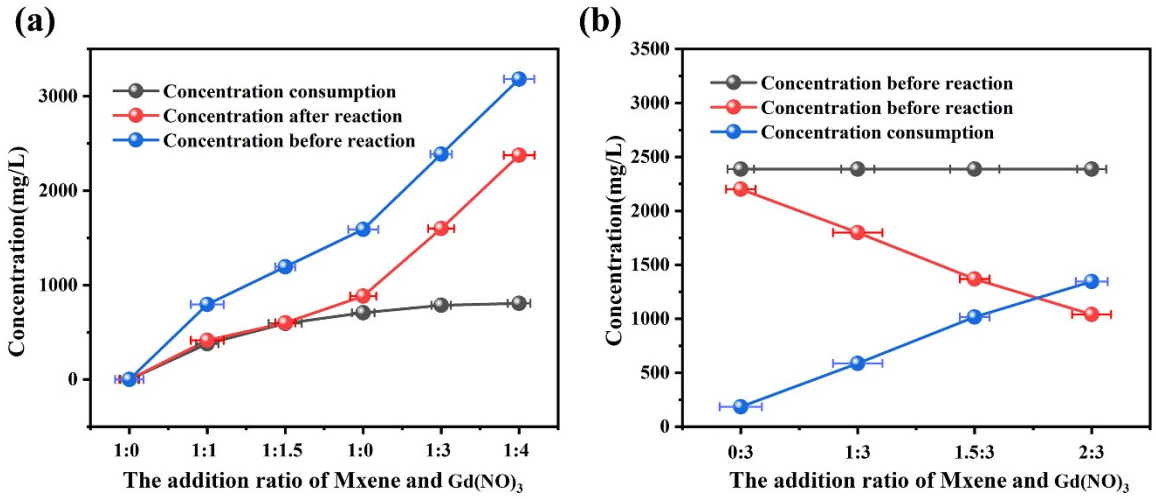

Fig. S4 The concentration of Gd^{3+} of concentration consumption, concentration after reaction, and concentration before reaction.

The calculation of the exact content $Gd(OH)CO_3$ and Gd_2O_3 in the GMNFs:

As shown in Fig. S5, during the first period of thermal analysis test (35 - 100 ℃), the mass loss of the MXene was mainly contributed to the volatilization of surface water. While in the second period of thermal analysis test (100 - 300 ℃), the evaporation of water between weak constraint layers was the main way of mass loss of the MXene, which mainly originated from water molecules that had hydrogen bonding interactions with MXene. The mass loss of the MXene in the third period (300 – 510 ℃) was mainly the removal of the MXene surface group (-OH and -F) by generating some molecules including H_2O and HF, and CO_2 released by oxidation reaction. During the fourth period of thermal analysis test (510 – 800 ℃), the mass loss of MXene was mainly contributed to the volatilization of bound water of MXene. For GMNFs, the mass loss of first, second, and third period was primarily the similar as MXene. Since the substance was easily decomposed at high temperature and produced H_2O and CO_2, the mass loss of the fourth period were contributed to the volatilization of the bound water and CO_2 of the decomposition of $Gd(OH)CO_3$. Based on this results, the exact content of $Gd(OH)CO_3$ in GMNFs (Table 2) could be obtained by subtracting the difference of mass loss of TG-FTIR experiment between MXene and GMNFs. The calculation process was shown in Table S2 of the supporting information.

First, the total content of Gd in GMNFs could be obtained from Fig. 4c, reaching 0.66%. Then the content of $Gd(OH)CO_3$ in GMNFs was obtained by comparing the types and contents of thermal decomposition products of GMNFs and MXene in the fourth stage of TG. In the fourth stage of TG, only H_2O was released from MXene as well as water and CO_2 were released in GMNFs. Therefore, the total amount of H_2O and CO_2 of $Gd(OH)CO_3$ could be obtained by

calculating the difference between the GMNFs and MXene. Moreover, the molar ratio of H_2O and CO_2 in $Gd(OH)CO_3$ was 1:1, and the mass of Gd was calculated by molar mass conversion: (2.87%-2.64%)*157/(44+18)=0.582%

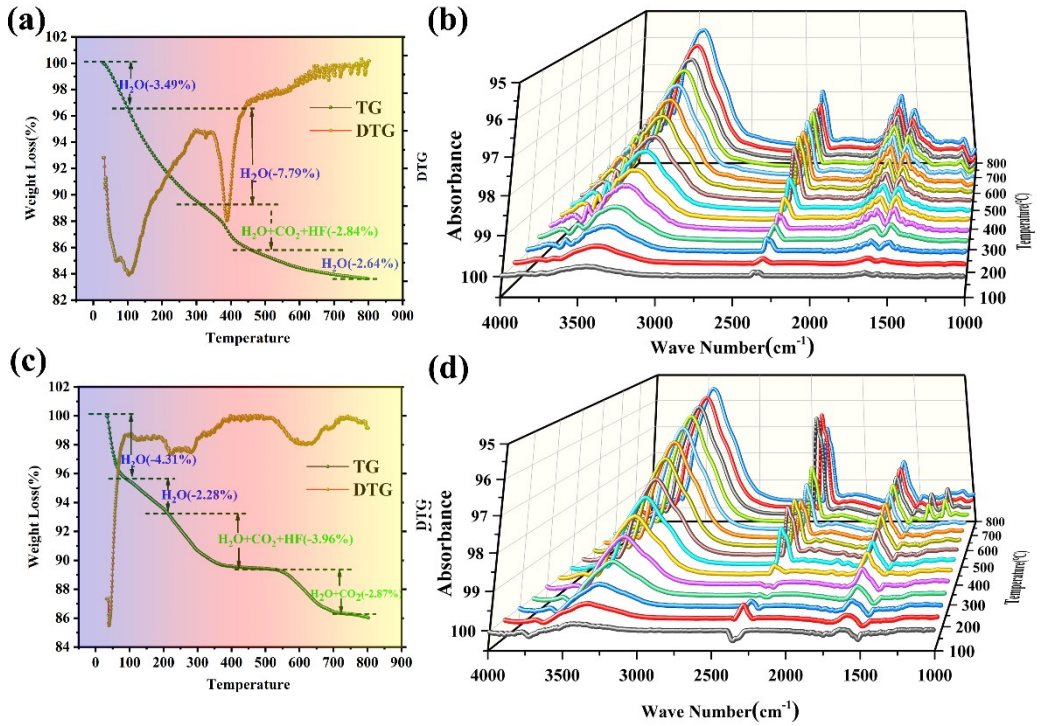

Fig. S5 Thermal weight analysis spectra (a) and TG-FTIR spectra of MXene (b). Thermal weight analysis spectra (c) and TG-FTIR spectra of 20-Gd@MXene (d).

Table S2 the exact content of $Gd(OH)CO_3$ and Gd_2O_3 of the GMNFs

	ω(Gd)	**ω(Gd in $Gd(OH)CO_3$)**	**ω(Gd in Gd_2O_3)**
GMNFs	**0.66%**	**0.582%**	**0.078%**

Comparison of the performance of this work with other works

It was well known that the shielding performance of neutron shielding materials was closely related to its thickness, and many studies had proved that the neutron shielding efficiency of materials improved with the increase of thickness[1-3].The thickness of the neutron shielding material prepared in this work was less than 100 μm. Due to the differences in the thickness of the materials between different works, and the thickness was a key factor affecting the neutron shielding performance of the material, it was necessary to specify a uniform thickness according to the relevant formula to compare shielding performance between different works. In the comparison of the neutron shielding efficiency of different works (Fig. S6), the thickness was uniformly calculated to 1mm.

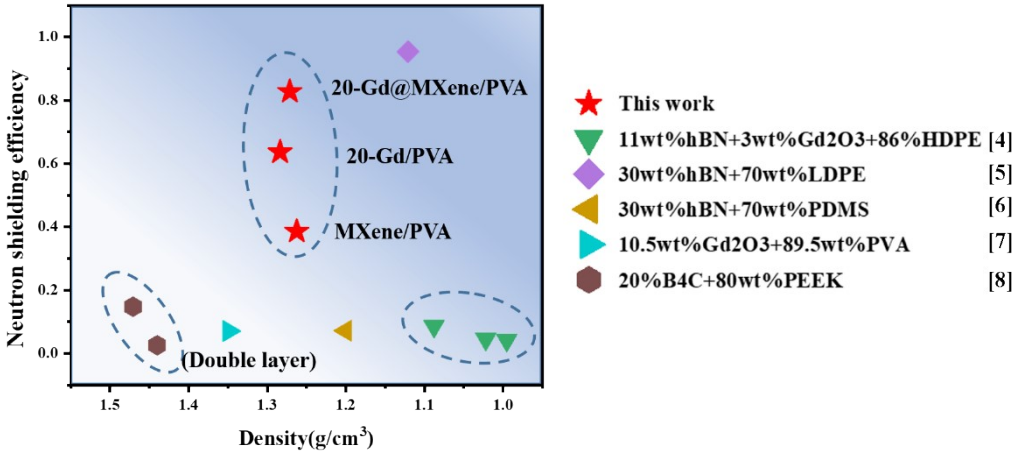

Fig. S6 Comparison of the performance of this work with other works[4-8].

The relationship between shielding efficiency and material thickness was as follows[9]:

$$\frac{I}{I_0} = exp(-\mu x) \quad \text{(S1-1)}$$

Where I was the intensity of neutron rays passing through the sample, I_0 was the initial neutron rays intensity; μ was the initial neutron rays intensity; x was the thickness of the shielding material.

$$\frac{\mu}{\rho} = \frac{1}{\rho x} ln(\frac{I_0}{I}) \quad \text{(S1-2)}$$

Where μ/ρ was the mass attenuation factor; I was the intensity of neutron rays passing through the sample, I_0 was the initial neutrons intensity; μ was the initial neutrons intensity; ρ was the density of the shielding material.

$$\mu = \frac{1}{x} ln(\frac{I_0}{I}) \quad \text{(S1-3)}$$

Where μ was linear attenuation coefficient; I was the intensity of neutron rays passing through the sample, I_0 was the initial neutrons intensity; μ was the initial neutrons intensity.

As shown in Fig. S6, compared with other works, this work showed a higher shielding efficiency under the thickness of 1 mm, reaching 83.1%. The excellent neutron shielding efficiency of this work was attributed to the perfect coordination of Gd NPs and MXene nanoflakes, and the related neutron shielding mechanism was shown in Fig. 9. Most of other works showed excellent shielding efficiency at a thickness of a few millimeters or centimeters, however, the neutron shielding efficiency was unsatisfactory when it extrapolated to a thickness of 1 mm. Compared with others, the advantage of this work was to achieve a more efficient neutron shielding efficiency with a lower filler ratio due to the clever structural of the filler.

References

1. J. W. Shin, J. W. Lee, S. Yu, B. K. Baek, J. P. Hong, Y. Seo, W. N. Kim, S. M. Hong and C. M. Koo, Thermochim. Acta, 2014, **585**, 5-9.
2. C. Harrison, S. Weaver, C. Bertelsen, E. Burgett, N. Hertel and E. Grulke, Journal of Applied Polymer Science, 2008, **109**, 2529-2538.
3. H. Chai, X. Tang, M. Ni, F. Chen, Y. Zhang, D. Chen and Y. Qiu, Journal of Nuclear Materials, 2015, **464**, 210-215.
4. T. Özdemir and S. N. Yılmaz, Radiation Physics and Chemistry, 2018, **152**, 93-99.
5. Y. Shang, G. Yang, F. Su, Y. Feng, Y. Ji, D. Liu, R. Yin, C. Liu and C. Shen, Composites Communications, 2020, **19**, 147-153.
6. Ş. G. İrim, A. A. Wis, M. A. Keskin, O. Baykara, G. Ozkoc, A. Avcı, M. Doğru and M. Karakoç, Radiation Physics and Chemistry, 2018, **144**, 434-443.
7. P. Tiamduangtawan, E. Wimolmala, R. Meesat and K. Saenboonruang, Radiation Physics and Chemistry, 2020, **172**, 108818.
8. Y. Wu, Y. Cao, Y. Wu and D. Li, 2020, **13**, 2314.
9. J. H. Hubbell, The International Journal of Applied Radiation and Isotopes, 1982, **33**, 1269-1290.